# Simulation study of UHECR particle propagation and photon fluxes

Daniel Kuempel[1a], Karl-Heinz Kampert[1], Markus Risse[1]

***Abstract*— We investigate ultra-high energy (UHE) particle propagation using the Monte Carlo code CRPropa. Particularly, the distance ranges from which particles of a certain energy reach the Earth, modifications of the spectra during propagation and photon fluxes, are studied for varying source parameters. First preliminary results are presented.**

## I. Introduction

One of the most pressing questions of astroparticle physics is the understanding of the origin and nature of the highest energy cosmic rays. Even though cosmic rays with energies exceeding $10^{20}$ eV have already been observed more than 40 years ago (e.g. [1]) many questions remain unanswered:

- "Where do they come from?"
- "What is their composition?"
- "What is the acceleration mechanism to such high energies which have already been observed?"
- "Is there an upper end in energy of the cosmic-ray flux?"
- ...

The discovery of the cosmic microwave background (CMB) radiation by Penzias and Wilson [2] 1965 lead Greisen [3] and independently Zatsepin and Kuzmin [4] 1966 to the point, that this radiation would make the Universe opaque to high energy protons, today known as the *GZK-suppression*[2]. They found that, above $\sim 5{\cdot}10^{19}$ eV, thermal photons are seen highly blue-shifted by the protons in their rest frames. The energy of the CMB photon is sufficient to excite baryon resonances thus draining energy of the primary nucleon resulting in a steepening of the energy spectrum. However, in spite of the prediction of the GZK-suppression, a number of experiments claimed to have observed events with $E > 10^{20}$ eV. Even before the cutoff was proposed in 1966, Volcano Ranch [5] observed one event. Later on, SUGAR [6] and Haverah Park [7] observed high energy events as well, but the interpretation is still disputed. Recently, both, the Yakutsk Array [8] and AGASA [9] have claimed to measure events above $10^{20}$ eV. The Yakutsk Array result seems to be in accordance with the GZK-suppression, but AGASA has claimed the opposite. The High Resolution Fly's Eye (HiRes) experiment claimed to observe the GZK-suppression [10]. HiRes observed two features in the ultra-high energy cosmic ray flux spectrum: The ankle at $4 \cdot 10^{18}$ eV and a high energy break in the spectrum at the energy of the GZK-suppression around $6 \cdot 10^{19}$ eV with a significance of about $5\sigma$. Recent results from the Pierre Auger Observatory [11] reject the hypothesis that the cosmic-ray spectrum continues with a constant slope above $4{\cdot}10^{19}$ eV, with a significance of more than $6\sigma$ [12].

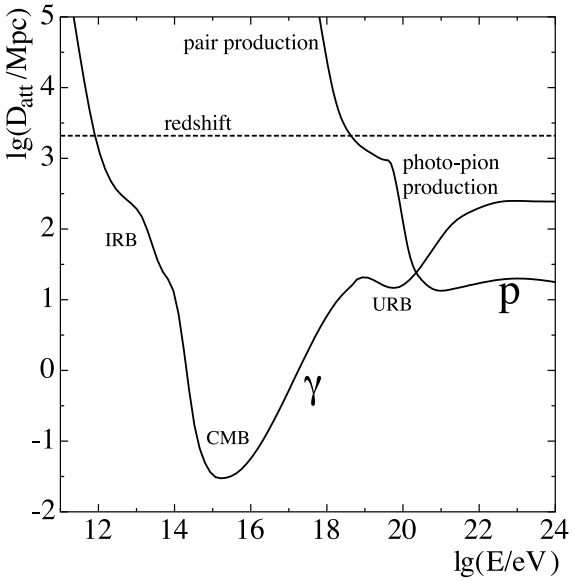


Fig. 1. Energy loss length of photons and protons for interactions with the photon background (cf. Ref. [13]).

Up to now the sources of ultra-high energy cosmic rays are still unknown. Recently, the Pierre Auger Observatory made an important step forward. They revealed a correlation between the arrival directions of ultra high energy cosmic rays (UHECR) with energy above $6 \cdot 10^{19}$ eV and the positions of active galactic nuclei (AGN) lying within $\sim 75 - 100$ Mpc [14]. At least if UHECR deflection in large scale cosmic magnetic fields is moderate, this requires a certain minimal density of sources within the "GZK-horizon" (cf. Sec. VI).

To get a clue of an answer of the raised questions it is therefore desirable to expand the knowledge of particle propagation through the local universe. The photon background is a key ingredient in understanding the properties of particle propagation. In the following, the most important energy loss mechanisms en route to Earth are discussed.

### A. Photo-Pion-production

For proton primaries, the most important interaction with the low-energy photon background is pion production, which

[1]Department of Physics, Bergische Universität Wuppertal, Gaußstr. 20, D-42097 Wuppertal, Germany, [a]kuempel@physik.uni-wuppertal.de

[2]In the literature this effect is also known as the GZK-Cutoff, although it is not a real cutoff.

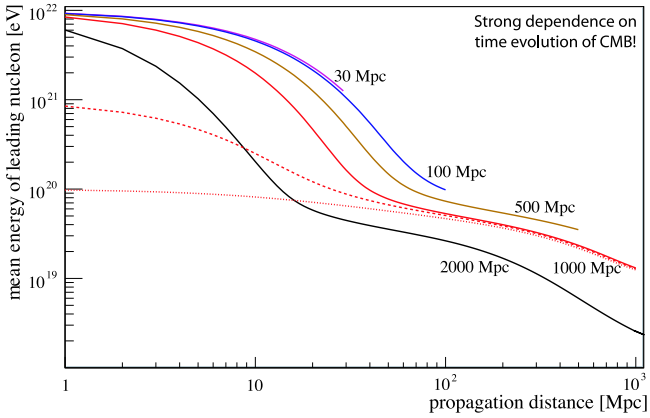


Fig. 2. Mean energy of the leading nucleon as a function of propagated distance. The dashed and dotted line represents a primary energy of $10^{21}$ and $10^{20}$ eV, respectively. Since the time evolution of the background photon spectra is taken into account, attenuation is stronger for distant (earlier in time) sources, as shown for $10^{22}$ eV initial energy events.

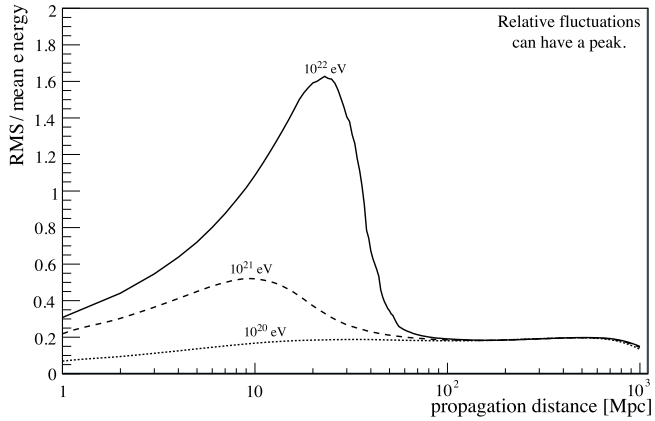


Fig. 3. Ratio of RMS fluctuations of energies to mean energy as a function of propagation distance (time) for the indicated initial energies (corresponding to the lines labeled 1000 Mpc in Fig. 2).

generates the already mentioned GZK feature. Here the low energy photon can Lorentz transform into a $\gamma$-ray in the rest frame of a very-high energy particle. The cross section is strongly increasing at the $\Delta^+(1232)$ resonance. The process can be described as

$$\begin{aligned} p + \gamma \rightarrow \Delta^+(1232) &\rightarrow n + \pi^+ \\ &\rightarrow p + \pi^0 \ . \end{aligned}$$

in addition, also further baryon resonances can occur with increasing energy:

$$p + \gamma_{\rm CMB} \rightarrow \Delta^{++} + \pi^- \rightarrow p + \pi^+ + \pi^- \ , \qquad (1)$$

where $\Delta^{++}$ indicates e.g. $\Delta(1620)$ or $\Delta(1700)$ resonances.

### B. Pair-production

Pair production by protons (also known as Bethe-Heitler process) on the low energy photon background is identical to the pair production interactions of $\gamma$-rays in the nuclear field and the dominant attenuation process below the GZK-suppression region. It can be described as

$$p + \gamma \rightarrow p + e^+ + e^- \ . \qquad (2)$$

The interaction length of this process is much shorter, compared to the photo-pion production, but on the other hand, the inelasticity is much lower, $\sim 10^{-3}$. This makes the pair production loss length of the order of Gpc (cf. Fig. 1).

### C. Redshift losses

The last important mechanism which dominates near and below the pair production threshold is redshifting due to the expansion of the universe. This adiabatic fractional energy loss can be described as

$$-\frac{1}{E}\left(\frac{{\rm d}E}{{\rm d}t}\right)_{\rm adiabatic} = H_0 \ , \qquad (3)$$

where $H_0$ is the present Hubble constant.

## II. CRPropa framework

The interplay between different astroparticle physics experiments has become very important. Existing and planned projects range from UHECR observations like the Pierre Auger Observatory, to neutrino telescopes [15], [16], as well as ground and space based $\gamma$-ray detectors operating at TeV and GeV energies, respectively [17]. Even if a putative source were to produce exclusively UHECRs, photo-pion and pair production by protons on the photon background would lead to guaranteed secondary photon and neutrino fluxes that could be detectable. With this motivation a numerical tool called CRPropa [18] has been developed that can treat the interface between UHECR, $\gamma$-ray and neutrino astrophysics, and large scale magnetic fields.

### A. Nucleon interactions

Pion production is modelled by using the event generator SOPHIA [19] that has been explicitly designed to study this phenomenon and is augmented in CRPropa for interactions with a low energy extra-galactic background light (EBL).

Unlike pion production, pair production by protons is taken into account as a continuous energy loss due to the low inelasticity. More details on the specific spectrum of the pairs and applied approximations are given in [18].

### B. Secondary electromagnetic cascades

The electromagnetic (EM) cascade code is based on [20]. All relevant interactions with a background photon are taken into account (cf. Fig. 1) and implemented in CRPropa including single pair production, double pair production, inverse Compton scattering and triplet pair production. If magnetic fields are selected, synchrotron losses of electrons are taken into account as well and the resulting lower energy synchrotron photons are also followed in the subsequent EM cascade.

### C. Background photon spectra and their evolution

There are three different photon backgrounds implemented in CRPropa. The most important is the CMB with a well

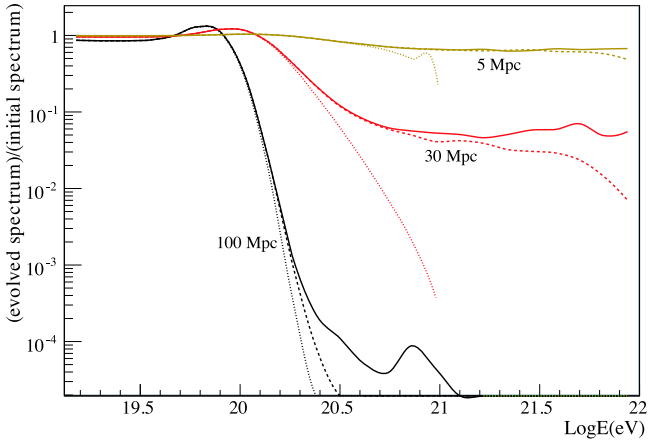


Fig. 4. Modification factor $f(E)$ of proton sources located at 100, 30 and 5 Mpc, respectively. The maximum simulated energy $E_{\rm max}$ is $10^{23}$ (solid line), $10^{22}$ (dashed line) and $10^{21}$ eV (dotted line). The "bump" preceding the GZK-suppression is more pronounced for distant sources. A plateau beyond the GZK-suppression becomes visible for larger $E_{\rm max}$ or closer distances. Note that the "wiggles" are indicative of the Monte Carlo statistics.

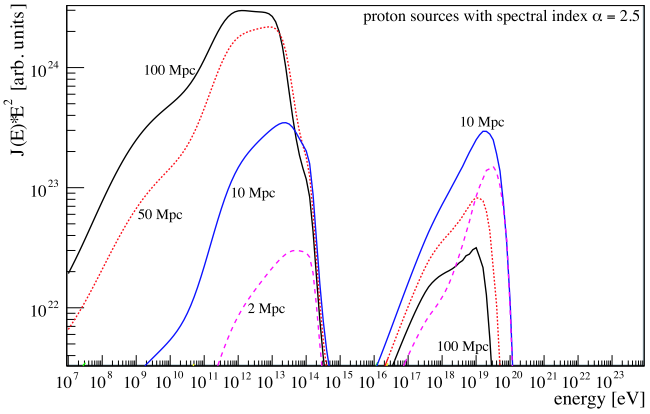


Fig. 5. Spectrum of secondary photons generated by pion and pair production from a single UHECR *proton* source at a given distance. We consider here a one-dimensional model, with an injection spectral index $\alpha$=2.5 and maximum energy of $10^{20.5}$ eV. No magnetic fields were taken into account. In this example, GZK-photons are mainly observed within a propagation distance of up to $25-50$ Mpc.

known redshift evolution. Three different infrared background (IRB) distributions can be chosen which are all consistent with recent limits from blazar observations. They become important for EM cascades around the threshold for pair production and are less significant in the UHE region. Above $\simeq 10^{18}$ eV interactions with the universal radio background (URB) become more important where it can inhibit cascade development due to the resulting small pair production length. The redshift evolution of the IRB and URB is more complicated and described in [18].

## III. Interactions en route to Earth

In the following we use a one dimensional simulation to calculate the attenuation of a primary proton when propagating through the intergalactic background light. All relevant energy losses (see above) are implemented. At a fixed distance from the observer, 60000 individual protons are injected and their energy loss is monitored with a stepsize of 1 Mpc. Three different primary energies of $10^{20}$, $10^{21}$ and $10^{22}$ eV are simulated. The mean energy of the leading nucleon as a function of propagation distance is shown in Fig. 2. After a distance of $\sim$100 Mpc the mean energy is essentially independent of the initial energy of the protons and that energy is less than $10^{20}$ eV. However, as a consequence of the time evolution of the CMB, the attenuation is stronger earlier in time with respect to a nearby source. This is shown for initial energies of $10^{22}$ eV where several distances (points in time) are illustrated. This effect starts to be significant at distances above 100 Mpc. The ratio of the RMS energy fluctuations to the mean energy as a function of propagation distance is shown in Fig. 3. For propagated distances in the range between $\sim 5-40$ Mpc, these fluctuations are very significant. They can give rise to deviations of a spectrum derived from a low number of events from the average spectrum (cf. Fig. 4), and should be taken into account when interpreting the observed spectrum.

## IV. Effect on observed spectra

The observed energy spectrum depends on the spatial distribution and the input spectrum of the sources. For the highest-energy part of the spectrum, the bulk of particles originates from relatively nearby sources (<100 Mpc) and hence the redshift evolution of the CMB and of the sources becomes negligible. In Fig. 4 the modification factor for different sources is illustrated. The modification factor $f(E)$ is given by

$$f(E) = \frac{I_p(E)}{I_0(E)} \ , \qquad (4)$$

where $I_0(E)$ is the injected spectrum and $I_p(E)$ is the spectrum as modified by the background light. As one can see, if the observed particles have an extragalactic origin, the interaction with the background light can dramatically change the original shape of accelerated particles injected into the intergalactic medium. By measuring the spectrum at highest energies the shape gives constrains on the maximum energy of the source (cf. Fig. 4). Moreover, the "bump" preceding the GZK-suppression is more pronounced for distant sources. A plateau beyond the GZK-suppression becomes visible for larger $E_{\rm max}$ or closer distances.

## V. Observed EM cascade

As described in Sec. II-B electromagnetic cascades are evolved and propagated to the observer. Fig. 5 illustrates the resulting spectra for a UHECR proton source at a given distance to the observer (with spectral index $\alpha = 2.5$). In this example, GZK-photons are mainly observed within a propagation distance of up to $25-50$ Mpc. Most of the contribution arises from nearby ($<25$ Mpc) sources with a peak at about 10 Mpc. More distant sources have the main

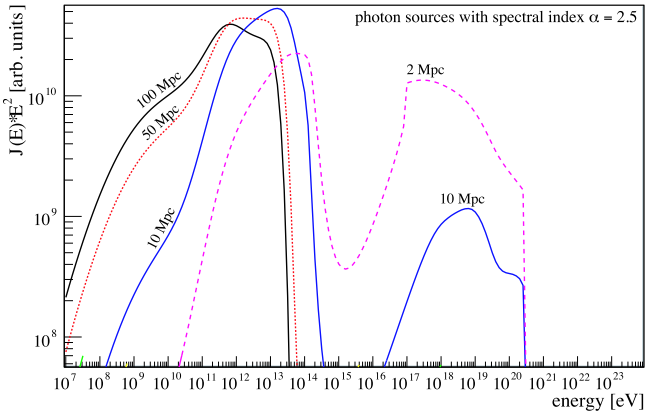


Fig. 6. Spectrum of secondary photons from a single UHECR *photon* source at a given distance. We consider here a one-dimensional model, with an injection spectral index $\alpha = 2.5$ and maximum energy of $10^{20.5}$ eV. No magnetic fields were taken into account.

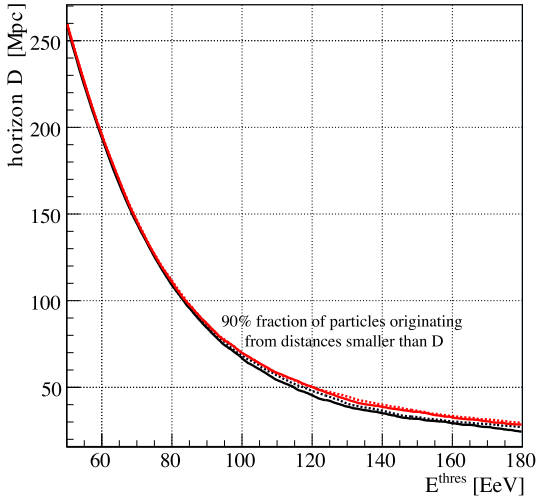


Fig. 7. GZK-horizon as a function of threshold energy for varying maximum energies of 500 EeV (solid, black), 1000 EeV (dotted, black), 1500 EeV (solid, red) and 10000 EeV (dotted, red).

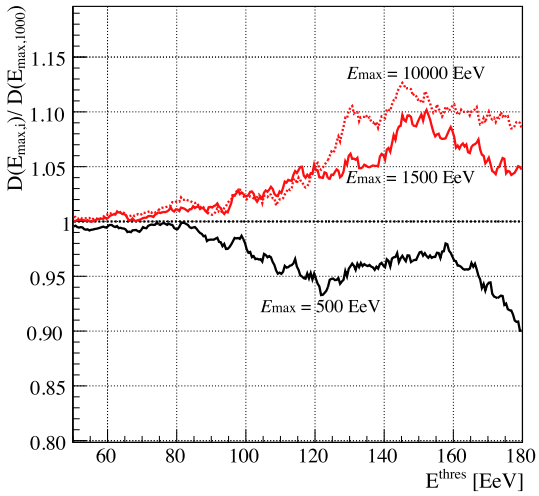


Fig. 8. Ratios of GZK-horizons shown in Fig. 7 normalized to $E_{\rm max} = 1000$ EeV. Larger $E_{\rm max}$ produce a more distant horizon for a growing energy threshold.

contribution in the TeV range. In Fig. 6 a photon source is assumed (also with spectral index $\alpha = 2.5$). At source distances close to the observer the largest EeV photon flux is expected.

## VI. GZK-HORIZON

Given the directional correlation of UHECR with relatively nearby AGN observed by the Pierre Auger Observatory [21], it is interesting to investigate the "GZK-horizon". The GZK-horizon reflects that distance, within which the major part of the observed events should be produced and is therefore an important parameter for anisotropy studies (cf. [21]). Within the present analysis the horizon is defined as the distance within which 90% of the observed events above a certain energy threshold $E^{\rm thres}$ were originally produced. In this simulation sources are distributed uniformly up to a distance of 800 Mpc. Unless stated otherwise, default values are $E_{\rm max} = 10^{21}$ eV, $\alpha = 2.7$ and $H_0 = 71$ km s$^{-1}$ Mpc$^{-1}$. The GZK-horizon as a function of threshold energy is shown in Fig. 7 for varying maximum energies. The calculated GZK-horizon at a threshold energy of $6 \cdot 10^{19}$ eV, where the correlation has maximum significance, is about 190 Mpc. This is to be compared with a value of $\sim 210$ Mpc from Ref. [22]. Compared to the distance $D_{\rm max} \simeq 75$ Mpc, where the correlation is most significant, a deviation of more than a factor 2 is observed. If these numbers were to be taken at face value, an upward shift in the energy calibration of $\sim 30\%$, as suggested in some simulations of the reconstruction of the shower energies [23], would lead to a better agreement between the maximum AGN distance $D_{\rm max}$ that maximises the correlation signal and the theoretical expectations based on the idealised GZK attenuation [21]. However, as also noted in Ref. [21], $D_{\rm max}$ may not directly be comparable to the GZK-horizon (for instance, an accidental correlation with foreground AGN different from the actual source may induce some bias in the value of $D_{\rm max}$ toward smaller maximum source distances).

The effect on different input parameters is shown in Figs. 8, 9 and 10. In Fig. 8 the effect on the maximum energy is shown. Larger $E_{\rm max}$ produce a more distant horizon for a growing energy threshold. Differences are of the order of $\sim 5\%$ for $E^{\rm thres} > 120$ EeV compared to the default values. Fig. 9 illustrates the effect of varying spectral indices of the source on the horizon. A more constant offset (energy independent) of about 2% is induced. The effect on the Hubble parameter $H_0$ is shown in Fig. 10. For lower energy thresholds, the effect seems to be of the order of $\sim 2\%$.

## VII. CONCLUSION

The interactions en route to earth of a primary proton/photon have been simulated using the Monte Carlo based propagation code CRPropa. There is a strong dependence on the evolution of the extragalactic background light in particular the CMB

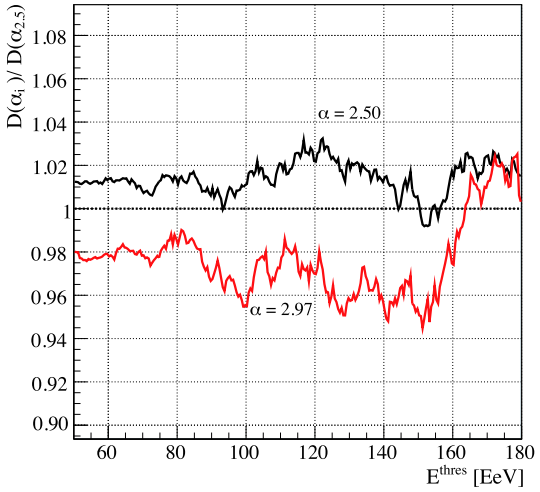


Fig. 9. Ratios of the GZK-horizon for varying spectral indices normalized to $\alpha = 2.7$. A spectral index of 2.5 (black) and 2.97 (red) is shown. Varying the spectral index induce a more constant (energy independent) offset in the horizon.

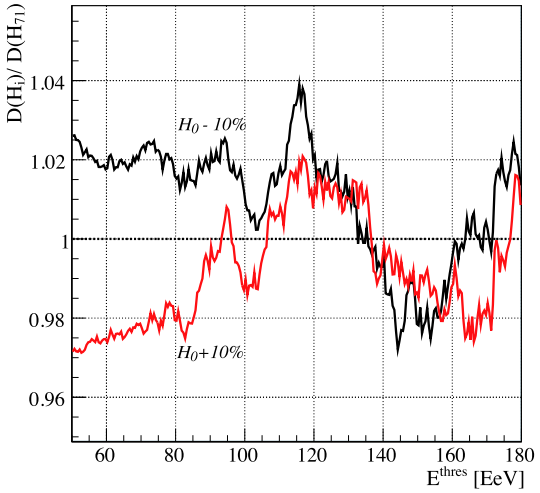


Fig. 10. Ratios of the GZK-horizon for a varying Hubble parameter normalized to $H_0 = 71$ km s$^{-1}$ Mpc$^{-1}$. A 10% variation H$-$10% (black) and $H_0+10\%$ (red) is shown. For lower energy thresholds the variations seems to dominate.

for distant sources ($> 100$ Mpc). Relative fluctuations are dominant in the range between $\sim 5-40$ Mpc and are important for a spectrum derived from a low number of events. GZK-photon fluxes of a proton source are mainly observed within a propagation distance of up to $25-50$ Mpc with a peak at about 10 Mpc. The effect of different input parameters on the GZK-horizon is investigated. For the maximum energy produced in the source, differences are of the order of $\sim 5\%$ above an energy threshold of $E^{\rm thres} \simeq 120$ EeV (cf. Fig. 8). There is a more constant (energy independent) offset for varying spectral indices. A variation of $\pm 10\%$ induces an offset of $\sim 2\%$ in the horizon. Furthermore a variation of $\pm 10\%$ of the Hubble parameter modifies the horizon of the order of $\sim 2\%$ for lower energy thresholds ($< 80$ EeV). Further investigations are in progress.

## Acknowledgements

We thank G. Sigl for fruitful discussions and suggestions related to the CRPropa framework. Helpful discussions with our Auger colleagues, particularly in our group in Wuppertal, are kindly acknowledged.
This work was partially supported by the German Ministry for Research and Education (Grant 05 A08PX1).

## References

[1] M. Nagano and A. A. Watson, Rev. Mod. Phys. **72** (2000) 689.
[2] A. A. Penzias and R. W. Wilson, "A Measurement of excess antenna temperature at 4080-Mc/s," *Astrophys. J.* **142** (1965) 419–421.
[3] K. Greisen, "End to the cosmic ray spectrum?," *Phys. Rev. Lett.* **16** (1966) 748–750.
[4] G. T. Zatsepin and V. A. Kuzmin, "Upper limit of the spectrum of cosmic rays," *JETP Lett.* **4** (1966) 78–80.
[5] J. Linsley, "Evidence for a primary cosmic-ray particle with energy $10^{20}$ eV," *Phys. Rev. Lett.* **10** (1963) 146–148.
[6] M. M. Winn, J. Ulrichs, L. S. Peak, C. B. A. Mccusker, and L. Horton, "The Cosmic Ray Energy Spectrum Above $10^{17}$ eV," *J. Phys.* **G12** (1986) 653–674.
[7] M. A. Lawrence, R. J. O. Reid, and A. A. Watson, "The Cosmic ray energy spectrum above $4{\cdot}10^{17}$ eV as measured by the Haverah Park array," *J. Phys.* **G17** (1991) 733–757.
[8] V. P. Egorova *et al.*, "The spectrum features of UHECRs below and surrounding GZK," *Nucl. Phys. Proc. Suppl.* **136** (2004) 3–11,
[9] M. Takeda *et al.*, "Energy determination in the Akeno Giant Air Shower Array experiment,". Prepared for 28th International Cosmic Ray Conferences (ICRC 2003), Tsukuba, Japan, 31 Jul - 7 Aug 2003.
[10] R. Abbasi *et al.* [HiRes Collaboration], Phys. Rev. Lett. **100** (2008) 101101
[11] J. Abraham *et al.* [Pierre Auger Collaboration], Nucl. Instrum. Meth. A **523** (2004) 50.
[12] J. Abraham *et al.* [Pierre Auger Collaboration], Phys. Rev. Lett. **101** (2008) 061101
[13] M. Risse and P. Homola, Mod. Phys. Lett. A **22** (2007) 749
[14] J. Abraham *et al.* [Pierre Auger Collaboration],22 Science **318** (2007) 938
[15] F. Halzen and D. Hooper, Rept. Prog. Phys. **65** (2002) 1025
[16] A. B. McDonald, C. Spiering, S. Schonert, E. T. Kearns and T. Kajita, Rev. Sci. Instrum. **75** (2004) 293
[17] H. J. Völk, arXiv:astro-ph/0312585.
[18] E. Armengaud, G. Sigl, T. Beau and F. Miniati, Astropart. Phys. **28** (2007) 463
[19] A. Mucke, R. Engel, J. P. Rachen, R. J. Protheroe and T. Stanev, Comput. Phys. Commun. **124** (2000) 290
[20] S. Lee, Phys. Rev. D **58** (1998) 043004
[21] J. Abraham *et al.* [Pierre Auger Collaboration], Astropart. Phys. **29** (2008) 188
[22] D. Harari, S. Mollerach and E. Roulet, JCAP **0611** (2006) 012
[23] R. Engel [Pierre Auger Collaboration], in Proceedings of the 30th International Cosmic Ray Conference, Mérida, México (2007), arXiv:0706.1921 [astro-ph]